Herrmann, A. M. et al. A novel method for the study of the biophysical interface in soils using nano-scale secondary ion mass spectrometry. Rapid Comm. Mass Spectrom. 21, 29-34

ARTICLE *in* RAPID COMMUNICATIONS IN MASS SPECTROMETRY · JANUARY 2007

Impact Factor: 2.25 · DOI: 10.1002/rcm.2811 · Source: PubMed

7 AUTHORS, INCLUDING:

Anke M Herrmann
Swedish University of Agricultural Sciences
32 PUBLICATIONS **536** CITATIONS
SEE PROFILE

Ian Robert Fletcher
Curtin University
138 PUBLICATIONS **4,493** CITATIONS
SEE PROFILE

Naoise Nunan
French National Centre for Scientific Resea…
84 PUBLICATIONS **2,039** CITATIONS
SEE PROFILE

Daniel Vaughan Murphy
University of Western Australia
134 PUBLICATIONS **4,005** CITATIONS
SEE PROFILE

RAPID COMMUNICATIONS IN MASS SPECTROMETRY
Rapid Commun. Mass Spectrom. 2007; **21**: 29–34
Published online in Wiley InterScience (www.interscience.wiley.com) DOI: 10.1002/rcm.2811

RCM

A novel method for the study of the biophysical interface in soils using nano-scale secondary ion mass spectrometry

Anke M. Herrmann[1,5*,†], Peta L. Clode[2], Ian R. Fletcher[2], Naoise Nunan[3], Elizabeth A. Stockdale[4], Anthony G. O'Donnell[5] and Daniel V. Murphy[1]

[1]School of Earth and Geographical Sciences, The University of Western Australia, 35 Stirling Highway, Crawley, WA 6009, Australia
[2]The Centre for Microscopy and Microanalysis, The University of Western Australia, 35 Stirling Highway, Crawley, WA 6009, Australia
[3]CNRS, UMR BioEMCo, Institut National Agronomique Paris-Grignon, Bâtiment EGER, 78850 Thiverval-Grignon, France
[4]School of Agriculture, Food and Rural Development, King George VI Building, University of Newcastle, Newcastle upon Tyne NE1 7RU, UK
[5]Institute for Research on Environment and Sustainability, Devonshire Building, University of Newcastle, Newcastle upon Tyne NE1 7RU, UK

Received 11 September 2006; Revised 26 October 2006; Accepted 27 October 2006

The spatial location of microorganisms and their activity within the soil matrix have major impacts on biological processes such as nutrient cycling. However, characterizing the biophysical interface in soils is hampered by a lack of techniques at relevant scales. A novel method for studying the distribution of microorganisms that have incorporated isotopically labelled substrate ('active' microorganisms) in relation to the soil microbial habitat is provided by nano-scale secondary ion mass spectrometry (NanoSIMS). *Pseudomonas fluorescens* are ubiquitous in soil and were therefore used as a model for 'active' microorganisms in soil. Batch cultures (NCTC 10038) were grown in a minimal salt medium containing ^{15}N-ammonium sulphate ($^{15/14}$N ratio of 1.174), added to quartz-based white sand or soil (coarse textured sand), embedded in Araldite 502 resin and sectioned for NanoSIMS analysis. The ^{15}N-enriched *P. fluorescens* could be identified within the soil structure, demonstrating that the NanoSIMS technique enables the study of spatial location of microbial activity in relation to the heterogeneous soil matrix. This technique is complementary to the existing techniques of digital imaging analysis of soil thin sections and scanning electron microscopy. Together with advanced computer-aided tomography of soils and mathematical modelling of soil heterogeneity, NanoSIMS may be a powerful tool for studying physical and biological interactions, thereby furthering our understanding of the biophysical interface in soils. Copyright © 2006 John Wiley & Sons, Ltd.

Soil microbial communities reside within a complex, heterogeneous physical structure that can have a significant impact upon a range of microbial processes by regulating access to substrate and oxygen,[1] by controlling diffusion of metabolites from microbial cells,[2,3] and by offering protection from environmental stresses[4] and predation.[5] Thus, the relationship between the spatial location of active soil microorganisms and the actual physical structure of the soil has a major influence on biological processes such as nutrient cycling. Given the heterogeneity of the soil matrix, external environmental conditions do not have a uniform effect throughout the soil, causing a large diversity of micro-habitats to develop.[6] Recent research has indicated that the distribution of microorganisms at the micro-scale and their interactions with the physical micro-habitat are non-random,[4,7,8] and has suggested that the micro-scale distribution of bacteria has a direct effect on their activity.[2,9] Although there is an increasing acceptance of the need to study the spatio-temporal patterns of soil processes at micro-scales in order to fully understand macro-scale behaviour (meter to landscape scales), few studies have attempted to address the spatial complexity of the soil with respect to biotic interactions and microbial process rates.[10]

A major obstacle to progress is the lack of techniques with adequate sensitivity for data collection at appropriate scales. To date, two methods, (i) a micro-sampling technique of specific microbial groups[11,12] and (ii) the universal fluorescent staining of soil bacteria combined with preparation of soil thin sections,[13–16] have been used for the study of the spatial distribution of microorganisms at the micro-scale. The advantage of the micro-sampling technique is that the three-dimensional spatial distribution of bacterial activity

*Correspondence to: A. M. Herrmann, Institute for Research on Environment and Sustainability, Devonshire Building, University of Newcastle, Newcastle upon Tyne NE1 7RU, UK.
E-mail: Anke.Herrmann@newcastle.ac.uk
† Present address: School of Earth and Geographical Sciences, The University of Western Australia, 35 Stirling Highway, Crawley, WA 6009, Australia.
Contract/grant sponsor: European Commission (Marie Curie Outgoing International Fellowship Scheme, FP6); contract/grant number: MOIF-CT-2005-00736.

and their functional significance can be studied.[11,12] It is not, however, possible to quantify the relationship between the spatial distribution of bacteria and soil structure. It is possible to quantify the relationship between microorganisms and other soil features using digital imaging analysis of soil thin sections,[7,15,17,18] but this approach does not distinguish between active and non-active microorganisms. Because the distribution of active microorganisms at the micro-scale may be of importance for a better understanding of nutrient cycling at the macro-scale,[2,19] there is a need for new analytical tools to quantify the spatial distribution of active microorganisms within the complex soil matrix.

Cliff *et al.*[20] showed that it was possible to qualitatively describe the assimilation of added ^{15}N and ^{13}C into soil microorganisms *in situ*, using time-of-flight secondary ion mass spectrometry (TOFSIMS), which provides data at the micro-scale. With the new generation of nano-scale secondary ion mass spectrometers (Cameca NanoSIMS),[21] the level of spatial resolution achievable is about 50 nm, a significant improvement on previous generations of SIMS instruments and on X-ray microanalytical techniques. To date, NanoSIMS has been principally applied to the study of extraterrestrial material[22–24] and in cell biology.[25–29] The high lateral resolution of NanoSIMS allows for subcellular tracking of isotopes in micron-sized unicellular organisms,[25,27,29] whilst the simultaneous detection of up to five different isotopic species with high sensitivity from the same soil microvolume means that micro-scale processes and interactions can be studied as never before. NanoSIMS microprobes have therefore the potential to explore factors that determine soil micro-site heterogeneity and to improve our understanding of links between the heterogeneous architecture of the soil matrix and the location of microbial activity.

The aim of this paper is to present the method and to show the potential of NanoSIMS for studying the distribution of microorganisms that have incorporated labelled substrate ('active' microorganisms) in relation to other soil characteristics such as the soil pore system and soil organic matter associated with the soil microbial habitat.

EXPERIMENTAL

Bacterial cultures

Pseudomonas fluorescens enriched with ^{15}N were used as a model for 'active' microorganisms as *Pseudomonas* species are ubiquitous in soil.[30] Batch cultures of *P. fluorescens* (NCTC 10038) were grown in a minimal salt medium (potassium dibasic phosphate 3.5 g/L; potassium monobasic phosphate 7.5 g/L; magnesium sulphate heptahydrate 0.05 g/L; sodium chloride 0.01 g/L; manganous sulphate monohydrate 4.58 mg/L; ferrous sulphate heptahydrate 0.55 mg/L; citric acid 0.75 mg/L; pH 7.2) containing 40 mM glucose-C and 15 mM ^{15}N-ammonium sulphate $(^{15}NH_4)_2SO_4$ ($^{15/14}N$ ratio of 1.174) to give a C/N ratio of 8. The glucose solution was filter sterilized through a 0.22 μm pore-size polycarbonate filter prior to use and the mineral medium with N source was autoclaved. The solutions were combined prior to inoculation. *P. fluorescens* were grown on an orbital shaker at 150 rpm at 25°C in the dark for 24 h. Mid-exponential-phase cells were harvested by centrifugation (12 000 rpm, 5 min) washed three times in 0.1 M sterile phosphate-buffered saline (pH 7.2), and resuspended in 1 mL to a cell density of 1.3×10^9 mL^{-1}.

Preparation of resin-embedded samples

A volume of 150 μL of this cell suspension was added to 1 g air-dry autoclaved quartz-based white sand or soil from the long-term claying experiment at Meckering, Western Australia (coarse textured sand with 1.1% soil C; 0.09% soil N; C/N ratio of 12; 120 μg C g^{-1} soil microbial biomass; pH of 6.5; 92% sand, 2.5% silt, 5.5% clay; mineralogy consists of quartz and kaolinite) and mixed thoroughly, resulting in a cell density of 2.8×10^8 g^{-1} soil . The method of preparing resin blocks was based on that of Nunan *et al.*[15] with some modifications. Directly after cell suspension addition, samples were inserted into a PVC cylinder (10 mm i.d., 4 cm long) sealed at the bottom with cheese cloth, repacked to a bulk density of 1.3 g cm^{-3} and immersed in an aqueous solution of 2.5% glutaraldehyde for 16 h at constant room temperature (21°C) so that the solution infused into the soil from the bottom. The samples were subsequently washed three times in deionized water for 10 min in the same manner, and then dried in a desiccator over silica gel at constant room temperature (21°C) for 1 week. To remove any residual water, the samples were transferred to a 30°C oven 24 h prior to resin impregnation.

To enable sample sectioning and NanoSIMS analysis, the samples were impregnated with vacuum-compatible epoxy resin. In a preliminary experiment, three blank mounts were prepared using different brands of resin (Araldite 502, ProSciTech, Kirwan, Qld, Australia; Buehler Epoxy, Biolab, Clayton, Vic, Australia; Korapox, Kömmerling Chemische Fabrik GmbH, Pirmasens, Germany), to determine their suitability for soil impregnation in this context. This was essentially a test of how well each of the resins filled the pore spaces in the soil and degassed through residual porosity. Araldite 502 proved the most suitable, giving the most rapid outgassing (i.e. releasing trapped and adsorbed gas rapidly, to enable pumping to the high vacuum required for NanoSIMS analysis; Fig. 1) and was therefore used to

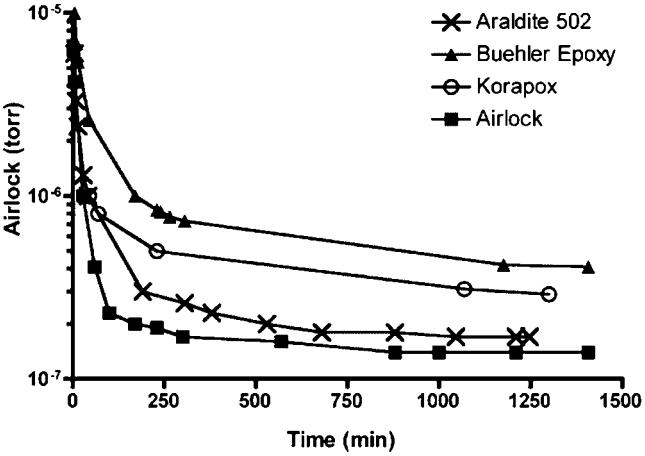

Figure 1. Outgassing of three blank resin mounts (Araldite 502, Buehler Epoxy and Korapox) over time, in the NanoSIMS airlock. Empty airlock vacuum levels are included for comparison.

DOI: 10.1002/rcm

prepare soil resin blocks. For resin impregnation, the samples were infiltrated from the bottom with Araldite 502 for at least 4 days; the first 24 h was under vacuum to aid resin penetration and to remove air bubbles. Resin-infiltrated samples were then cured under vacuum for 36 h. Finally, the samples were sawn into 2 mm thick slices, polished and coated with 5 nm gold for NanoSIMS analysis. In terms of reproducibility, two or three sections were prepared from each of six soil resin blocks. All sections were found to be suitable for NanoSIMS analysis.

Cameca NanoSIMS50® ion microprobe

All data were acquired with the Cameca NanoSIMS50® instrument (Cameca, Gennevilliers, France) using a $[Cs]^+$ primary ion probe, with 16 kV primary ion impact energy and 8 kV secondary ion extraction voltage. Four electron-multiplier secondary ion collectors were used, with 75 μm exit slits for $[^{12}C]^-$, $[^{12}C^{14}N]^-$, $[^{12}C^{15}N]^-$ and $[^{28}Si]^-$. The majority of ion images, including the mosaics (see below), were acquired using a ~0.9 pA primary ion current (D1-2 primary beam aperture), a ~0.5 μm probe diameter and integration times typically ~10 ms/pixel. Higher resolution images (field of view = 10 μm) were obtained using a ~0.1 pA primary ion current (D1-5 primary beam aperture), a ~100 nm probe diameter and integration time of 50 ms/pixel. The additional NanoSIMS tuning required for optimum spatial resolution (i.e. ~50 nm probe diameter) was not justified because no materials in the sample were suitable for doing so at low primary ion beam current. The mass resolution was ~5000 (MRP, Cameca definition). Under these conditions, complete separation of the isobars from $[^{12}C^{14}N]^-$ and $[^{12}C^{15}N]^-$ was not possible, but interference effects were <2 orders of magnitude for the target molecular isotopes in the ^{15}N-enriched *P. fluorescens*. Cliff *et al.*[20] have reported isobaric interference of $[^{27}Al]^-$ with $[^{13}C^{14}N]^-$ and $[^{12}C^{15}N]^-$ when analyzing soil using a $[Ga]^+$ primary ion probe with TOFSIMS. Such interferences are not an issue in NanoSIMS analysis as aluminium does not ionize very easily with a $[Cs]^+$ primary ion probe and thus the yield of these ions is negligible.

Mosaics of ion images (total field of view of 270 × 150 μm) were made to allow the study of biophysical interactions in soils at relevant scales. The nominal image size was 30 μm square and the step between images was 25 μm, deliberately less than the image frame size to ensure that the entire imaged areas were Cs-implanted before recording, and to facilitate mosaic construction. Implantation of $[Cs]^+$ prior to analysis was necessary to remove most of the gold coat and surface-adsorbed N and C, and to stimulate secondary ion emission. This was achieved by a 'dummy' imaging step using a high primary beam current (D1-1 aperture).

Maps representing $^{15/14}N$ ratios were obtained by dividing the $[^{12}C^{15}N]^-$ counts by $[^{12}C^{14}N]^-$ counts for each pixel, using the MIMS plug-in for the freeware package, Image J.[31] To demonstrate the discriminatory power of the method, numerical $^{15/14}N$ ratio data were extracted directly from these $[^{12}C^{15}N]^-/[^{12}C^{14}N]^-$ images by drawing regions of interest (ROIs) on the ratio image. Each ROI was drawn three times to obtain a mean ratio from any given area. Mean area and ratio ± standard errors of the mean as well as maximum and minimum $^{15/14}N$ ratios for each ROI are reported. Line scan data (length = 8 μm) were also extracted using Image J.[31] For integration of the biophysical interface in soil, ion images of $[^{28}Si]^-$, $[^{12}C^{14}N]^-$ and the $^{15/14}N$ ratio data were then superimposed using Digital Micrograph (Gatan Inc., Pleasanton, CA, USA). For comparison, cell suspensions (80 μL; three replicates) of *P. fluorescens* without soil were dried in a desiccator over silica gel at 40°C overnight (16 h) and their $^{15/14}N$ ratio was determined using an automated Roboprep C/N analyzer coupled with a Europa Scientific VG Micromass Sira 9 mass spectrometer (ANCA-MS: SerCon Australia PTY Ltd., Fulham Gardens, SA, Australia).

SEM imaging and X-ray microanalysis

Before NanoSIMS analyses could be performed, all soil mounts were imaged using a Zeiss 1555 VP field emission scanning electron microscope (Carl Zeiss, Oberkochen, Germany) to identify potentially suitable areas for NanoSIMS analysis. After NanoSIMS analyses, samples were re-coated with 10 nm carbon and returned to the scanning electron microscope. Regions previously analyzed by NanoSIMS were imaged and further analyzed using energy dispersive spectroscopy (EDS) X-ray microanalysis. Backscattered electron imaging was performed at 25 kV and qualitative EDS X-ray maps of silica were acquired at 20 kV, using Isis X-ray software (Oxford Instruments, Penant Hill, NSW, Australia).

RESULTS AND DISCUSSION

Map of ^{15}N-enriched *P. fluorescens* mixed into quartz-based white sand

Typical secondary ion images of $[^{28}Si]^-$, $[^{12}C]^-$, $[^{12}C^{14}N]^-$ and the $^{15/14}N$ ratio image from ^{15}N-labelled *P. fluorescens* mixed into quartz-based white sand are presented in Fig. 2. The $[^{28}Si]^-$ ion image provides information on the sand matrix (Fig. 2(a)), while resin distribution is revealed in both the $[^{12}C]^-$ and $[^{12}C^{14}N]^-$ ion images (Figs. 2(b) and 2(c)); Araldite contains 72.6% C and 0.7% N. Nitrogen-rich organic matter is also clearly visible in the $[^{12}C^{14}N]^-$ ion image, as the ^{14}N signal from resin is uniformly low and does not mask these signals (Figs. 2(c) and 5(b)). The distribution and level of ^{15}N are presented in the $^{15/14}N$ ratio image (Fig. 2(d)), which clearly depicts the ^{15}N-enriched *P. fluorescens* aligned along edges of sand particles. These bacteria were highly enriched in ^{15}N in comparison with natural abundance (Fig. 2(d)).

Maps of ^{15}N-enriched *P. fluorescens* mixed into coarse textured sand

Superimposed ion distribution images of $[^{28}Si]^-$, $[^{12}C^{14}N]^-$ and the $^{15/14}N$ ratio of ^{15}N-enriched *P. fluorescens* mixed into a coarse textured sand are given in Fig. 3(a). Blue, green and red colours represent the distribution of the $[^{28}Si]^-$, $[^{12}C^{14}N]^-$ and $^{15/14}N$ ratio, respectively. As illustrated by this high-resolution image (Fig. 3(a)), the spatial distribution of ^{15}N-enriched bacteria (i.e. $^{15/14}N$ ratio image, red colour) in relation to the soil matrix (i.e. $[^{28}Si]^-$ ion image, blue colour) and the soil organic matter (i.e. $[^{12}C^{14}N]^-$ ion image,

DOI: 10.1002/rcm

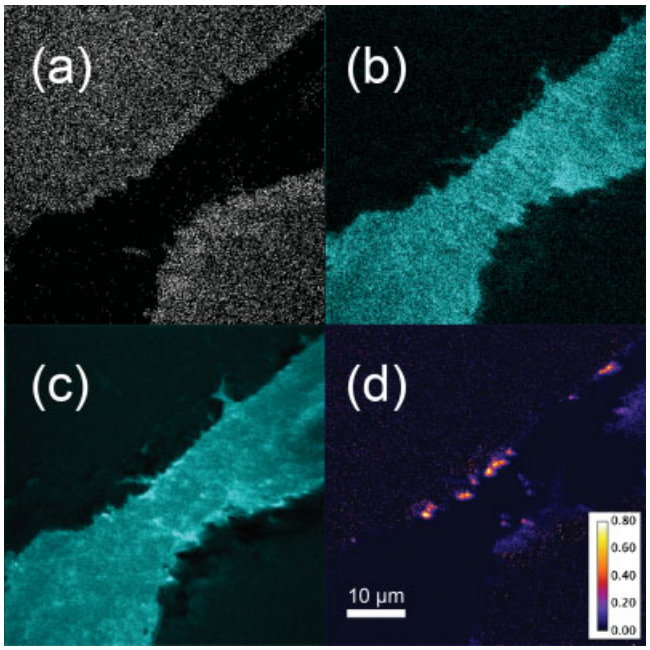

Figure 2. Typical NanoSIMS images of a cross section of ^{15}N-labelled *P. fluorescens* mixed in quartz-based white sand and embedded in Araldite resin: (a) $[^{28}Si]^-$; (b) $[^{12}C]^-$; (c) $[^{12}C^{14}N]^-$; and (d) $^{15/14}$N ratio (field of view = 55 μm). Scale on (d) indicates $^{15/14}$N ratio values.

green colour) can readily be studied at previously unattainable small scales as the ^{14}N signal from resin is uniformly low (Figs. 2(c) and 5(b)) and does not mask these signals.

This high-resolution image also allows for verification of ^{15}N-enrichment in *P. fluorescens*. The five individual bacteria identified by ion imaging (shown in Fig. 3(b)) were all significantly ^{15}N-enriched ($P < 0.05$, Mann-Whitney test) in comparison with the resin which gave a $^{15/14}$N ratio of 0.0043 ± 0.0002 (standard error, SE) (Table 1). These values obtained from resin-only regions are essentially indistinguishable from natural ^{15}N terrestrial values ($^{15/14}$N natural abundance = 0.0037), given the possibility of minor unresolved isobars. High variability of the $^{15/14}$N ratio can be seen within individual bacteria, evident in the wide range of maxima and minima within each ROI (Table 1) and the line scan data (Fig. 4), sampled across two ^{15}N-enriched *P. fluorescens*, which had been identified by ion imaging (Fig. 3(b)). The wide range of values in each ROI can be explained either by differential accumulation of ^{15}N in the cells or by ion signals from the outside of each ROI contributing to the low minimum $^{15/14}$N ratio. The latter is unavoidable when analyzing small ROIs due to the finite size of the primary ion beam. The average $^{15/14}$N ratio of the labelled bacteria was 0.520 ± 0.035 (SE) with no significant differences ($P < 0.05$, Kruskal Wallis analysis of variance (ANOVA)) between the five individual bacteria (Fig. 3(b) and Table 1) or the $^{15/14}$N ratio from resin-embedded *P. fluorescens* prepared without soil (data not shown). Thus, there appeared to be no interference from the soil matrix in determining ^{15}N enrichment. As the $^{15/14}$N ratios from resin were in accordance with expected natural abundances, we

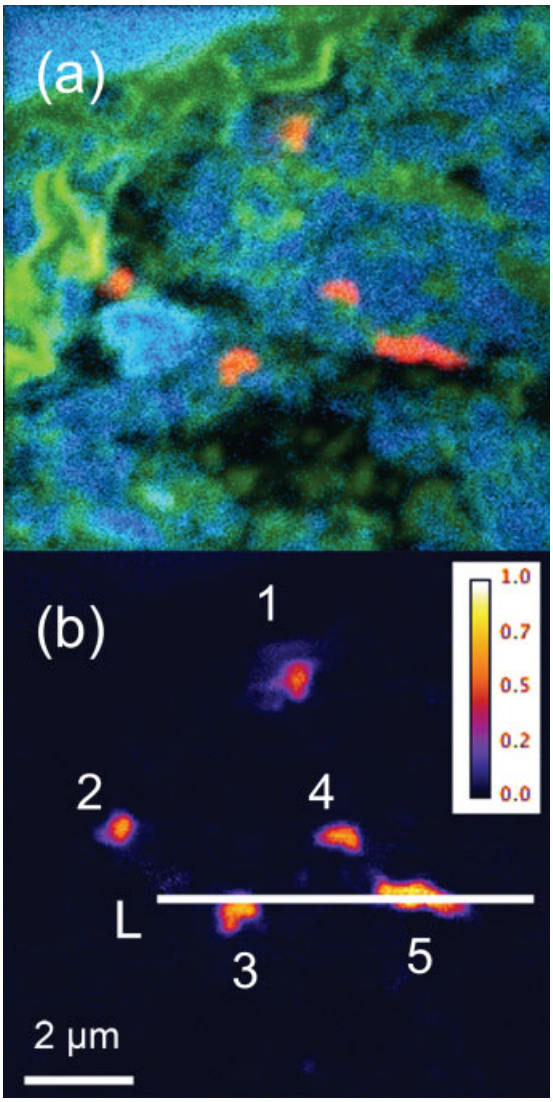

Figure 3. (a) Superimposed NanoSIMS images (blue = $[^{28}Si]^-$; green = $[^{12}C^{14}N]^-$ and red = $^{15/14}$N ratio) and (b) $^{15/14}$N ratio image only with depicted region of the linescan (L) of a cross section of ^{15}N-labelled *P. fluorescens* mixed in coarse textured sand and embedded in Araldite resin (field of view = 10 μm).

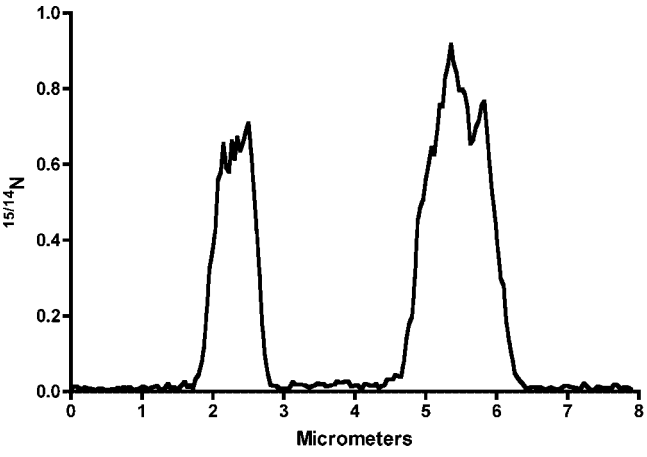

Figure 4. Linescan data using the MIMS plug-in for the freeware package, Image J.[31] The trace of the linescan (L) is depicted in Fig. 3(b).

DOI: 10.1002/rcm

Table 1. Region of interest (ROI) data detailing $^{15/14}$N ratios of ^{15}N-enriched *Pseudomonas fluorescens*. Data were extracted directly from NanoSIMS $^{15/14}$N ratio images and ROIs correspond to those depicted in Fig. 3(b). Mean area of ROI (μm^2), mean $^{15/14}$N ratio and standard errors of the means

ROI	Area of ROI mean (μm^2)	Mean $^{15/14}$N ratio	Maximum $^{15/14}$N ratio	Minimum $^{15/14}$N ratio
1	0.185 ± 0.015	0.418 ± 0.007	0.619	0.212
2	0.130 ± 0.007	0.491 ± 0.014	0.685	0.262
3	0.208 ± 0.012	0.557 ± 0.007	0.777	0.278
4	0.178 ± 0.018	0.508 ± 0.012	0.746	0.211
5	0.467 ± 0.026	0.628 ± 0.014	0.994	0.257
Resin	10.46 ± 1.29	0.0043 ± 0.0002	—	—

can be certain that our ^{15}N data and the levels of enrichment measured are accurate. The $^{15/14}$N ratio of cell suspensions of *P. fluorescens* was 0.82 ± 0.04 (SE) when determined on an isotope ratio mass spectrometer (ANCA-MS). Therefore, in comparison, *P. fluorescens* mixed into coarse textured sand contained maximum levels of ^{15}N (Table 1 and Fig. 4) similar to the $^{15/14}$N ratio of the enriched bacteria in cell suspensions, indicating that only a small amount of ^{15}N may have been removed during sample processing.

In comparison, Clode *et al.*[29] reported that only 35% of photosynthetically fixed ^{13}C was retained as protein in symbiotic algae, following chemical fixation in a glutaraldehyde/paraformaldehyde mixture. The differences between preserving C and N at different levels within cells after chemical fixation can be explained by the fact that glutaraldehyde reacts with amine groups, stabilizing material by cross linking proteins, purines and pyrimidines, making them insoluble and immobile.[32] As cellular N in bacteria is primarily in proteins and nucleic acids it is stabilized by chemical fixation. On the other hand, the C fixed as a result of photosynthesis may be lost during subsequent treatment as small soluble molecules such as sugars, which are not stabilized with glutaraldehyde. Clode *et al.*[29] therefore concluded that low-temperature methods, such as freeze-drying, might offer a more promising solution.[33,34] This approach has been successfully used to study ^{13}C and ^{15}N metabolism in cultured cells using NanoSIMS.[25] However, the preparation method of choice will ultimately depend on the nature of the sample, the compound of interest, the availability of equipment and question to be addressed. In many cases, more than one preparation technique may be needed. In our case, chemical fixation appears to be a suitable method for studying ^{15}N accumulation in *P. fluorescens*.

Mapping the biophysical interface in soil

Mosaics of superimposed $^{28}[Si]^-$ and $^{15/14}$N ratio images (Fig. 5(a)) and $[^{12}C^{14}N]^-$ and $^{15/14}$N ratio images (Fig. 5(b)) are presented along with a backscattered electron image (Fig. 5(c)) and a qualitative EDS X-ray silica map of the same area (Fig. 5(d)). The silica distributions in the EDS X-ray map (Fig. 5(d)) and the $^{28}[Si]^-$ mosaic (Fig. 5(a)) are concordant, emphasizing that NanoSIMS analysis gives reliable silica distribution. Spatial distributions of the soil matrix and organic matter are given in the mosaics of the $[^{28}Si]^-$ (Fig. 5(a)) or $[^{12}C^{14}N]^-$ ion images (Fig. 5(b)), respectively.

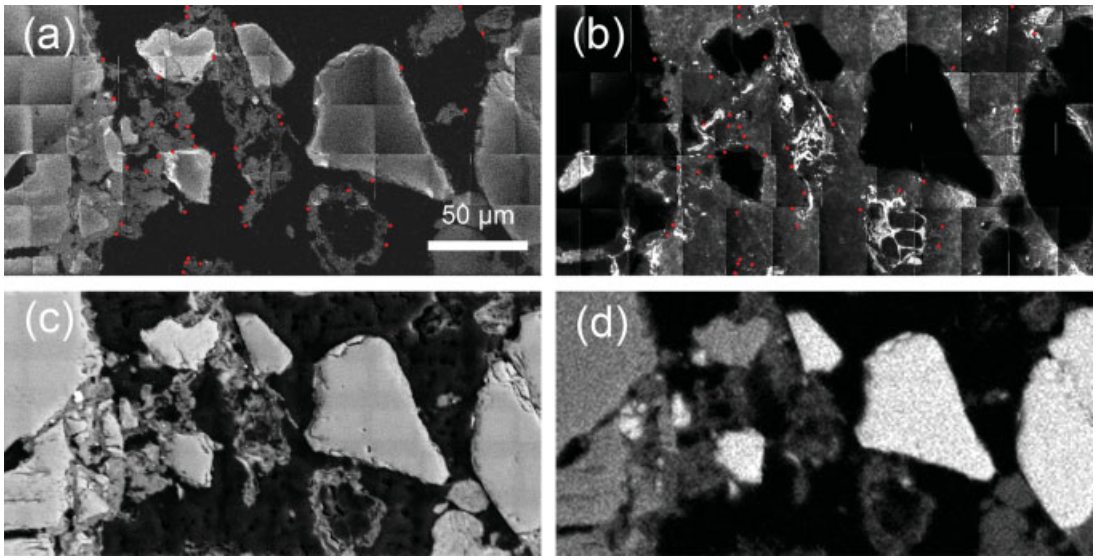

Figure 5. Cross section of ^{15}N-labelled *P. fluorescens* mixed in coarse textured sand: mosaic of (a) $[^{28}Si]^-$ ion images or (b) $[^{12}C^{14}N]^-$ ion images, superimposed with $^{15/14}$N ratio images (red points denote ^{15}N enriched microorganisms, i.e. $^{15/14}$N ratio images, as these bacteria were too small to be distinguished at the scale of the mosaic) (field of view = 30 µm for each ion image and step between images of 25 µm giving a total field of view of 270×150 µm). (c) Backscattered electron image and (d) qualitative EDS X-ray silica map using a Zeiss 1555 VP field emission scanning electron microscope (field of view = 270×150 µm).

DOI: 10.1002/rcm

The ^{15}N-enriched bacteria were, however, too small to be distinguished at the scale of the mosaic, but they can be readily identified in the individual ion image frames (e.g. Figs. 2 and 3). For illustrative purpose, oversized red points were therefore used to denote ^{15}N-enriched microorganisms associated with the $[^{28}Si]^-$ (Fig. 5(a)) and $[^{12}C^{14}N]^-$ (Fig. 5(b)) matrices.

As exemplified in the two mosaics (Fig. 5) and the high-resolution image in Fig. 3, the NanoSIMS ion microprobe can be used to study ^{15}N-enriched bacteria in relation to soil characteristics such as the soil matrix and organic matter over both a reasonably large (270–150 μm field of view) and a very small (10 μm field of view) scale. This new technique has therefore the potential to examine microbial nitrogen metabolism *in situ* in relation to the soil microbial habitat which was hitherto not feasible.

CONCLUSIONS

This work has demonstrated the potential of NanoSIMS, the new generation of ion microprobe, to explore the biophysical interface in soils. NanoSIMS analysis is not restricted to N isotopes, as most elements (e.g. C, O, P) and their isotopes can be analyzed with very high sensitivity. However, it has to be borne in mind that NanoSIMS can only analyze a limited area and therefore existing methods such as digital imaging analysis of thin sections[7,15,17,18] and scanning electron microscopy are required to identify regions of interest. Together with advanced computer-aided tomography of soils[6] and mathematical modelling of soil heterogeneity,[35] NanoSIMS may be a powerful tool for studying physical and biological interactions thereby furthering our understanding of the biophysical interface in soils.

Acknowledgements

Thanks are extended to Dr Richard Stern for providing resin degassing data, Dr Charlene Kahler for assistance with determining bacterial cell densities and Mr Frank Nemeth for sawing soil resin blocks. We thank the European Commission (Marie Curie Outgoing International Fellowship Scheme FP6) for financial support. This research was carried out using facilities at the Centre for Microscopy and Microanalysis, The University of Western Australia, which are supported by University, State and Federal Government funding. The Cameca NanoSIMS50 facility was funded by a Major National Research Facility (MNRF) grant through the Nanostructural Analysis Network Organisation (NANO).

REFERENCES

1. Sierra J, Renault P, Valles V. *Eur. J. Soil Sci.* 1995; **46**: 519.
2. Strong DT, Sale PWG, Helyar KR. *Aus. J. Soil Res.* 1997; **35**: 565.
3. Chenu C, Hassink J, Bloem J. *Biol. Fertil. Soils* 2001; **34**: 349.
4. Ranjard L, Poly F, Combrisson J, Richaume A, Gourbiere F, Thioulouse J, Nazaret S. *Microb. Ecol.* 2000; **39**: 263.
5. Young IM, Ritz K. *Soil Biol. Biochem.* 1998; **30**: 1229.
6. Nunan N, Ritz K, Rivers M, Feeney DS, Young IM. *Geoderma* 2006; **133**: 398.
7. Nunan N, Wu K, Young IM, Crawford JW, Ritz K. *FEMS Microb. Ecol.* 2003; **44**: 203.
8. Mummey DL, Stahl PD. *Microb. Ecol.* 2004; **48**: 41.
9. Pallud C, Dechesne A, Gaudet JP, Debouzie D, Grundmann GL. *Appl. Environ. Microbiol.* 2004; **70**: 2709.
10. Young IM, Crawford JW. *Science* 2004; **304**: 1634.
11. Grundmann GL, Dechesne A, Bartoli F, Flandrois JP, Chasse JL, Kizungu R. *Soil Sci. Soc. Am. J.* 2001; **65**: 1709.
12. Dechesne A, Pallu C, Debouzie D, Flandrois JP, Vogel TM, Gaudet JP, Grundmann GL. *Soil Biol. Biochem.* 2003; **35**: 1537.
13. White D, Fitzpatrick EA, Killham K. *Geoderma* 1994; **63**: 245.
14. Fisk AC, Murphy SL, Tate RL. *Biol. Fertil. Soils* 1999; **28**: 111.
15. Nunan N, Ritz K, Crabb D, Harris K, Wu K, Crawford JW, Young IM. *FEMS Microb. Ecol.* 2001; **36**: 67.
16. Li Y, Dick WA, Tuovinen OH. *Biol. Fert. Soils* 2004; **39**: 301.
17. Harris K, Young IM, Gilligan CA, Otten W, Ritz K. *FEMS Microbiol. Ecol.* 2003; **44**: 45.
18. Bruneau PMC, Davidson DA, Grieve IC, Young IM, Nunan N. *FEMS Microbiol. Ecol.* 2005; **52**: 139.
19. Strong DT, De Wever H, Merckx R, Recous S. *Eur. J. Soil Sci.* 2004; **55**: 739.
20. Cliff JB, Gaspar DJ, Bottomley PJ, Myrold DD. *Appl. Environ. Microbiol.* 2002; **68**: 4067.
21. Slodzian G, Daigne B, Girard F, Boust F, Hillion F. *Biol. Cell* 1992; **74**: 53.
22. Messenger S, Keller LP, Stadermann FJ, Walker RM, Zinner E. *Science* 2004; **300**: 105.
23. Floss C, Stadermann FJ, Bradley J, Dai ZR, Bajt S, Graham G. *Science* 2004; **300**: 1355.
24. Hoppe P, Ott U, Lugmair GW. *New Astronomy Rev.* 2004; **48**: 171.
25. Peteranderl R, Lechene C. *J. Am. Soc. Mass Spectrom.* 2004; **15**: 478.
26. Kleinfeld AM, Kampf JP, Lechene C. *J. Am. Soc. Mass Spectrom.* 2004; **15**: 1572.
27. Guerquin-Kern JL, Hillion F, Madelmont JC, Labarre P, Papon J, Croisy A. *BioMedical Eng. OnLine* 2004; **3**: 1.
28. Hallegot P, Peteranderl R, Lechene C. *J. Invest. Dermatol.* 2004; **122**: 381.
29. Clode PL, Stern RA, Marshall AT. *Micros. Res. Tech.* 2007; in press.
30. Krieg NR, Holt JG. *Bergey's Manual of Systematic Bacteriology*, vol. **1**. William and Wilkins: Baltimore, 1984.
31. Available: http://rsb.info.nih.gov/ij/ (accessed 2006).
32. Nougarède A. *Précis de Sciences Biologiques. Biologie Végétale I, Cytologie*. Masson: Paris, 1969.
33. Chandra S, Sod EW, Ausserer WA, Morrison GH. *Pure Appl. Chem.* 1992; **64**: 254.
34. Echlin P. *Low Temperature Microscopy and Analysis*. Plenum Press: New York, 1992.
35. Wu KJ, Nunan N, Crawford JW, Young IM, Ritz K. *Soil Sci. Soc. Am. J.* 2004; **68**: 346.

DOI: 10.1002/rcm